A Pseudobubblepoint Model and Its Simulation for Foamy Oil in Porous Media

Zhangxin Chen and **Jian Sun,** University of Calgary,
Ruihe Wang, China National Oil and Gas Exploration and Development Corporation, and
Xiaodong Wu, Petroleum University of China, Beijing

Summary

This is the second paper of a series in which we study heavy oil in porous media. The first paper dealt with an experimental study (Wang et al. 2008), whereas a mathematical and simulation study is presented here. The research program stems from the need to predict the field performance of a class of heavy-foamy-oil reservoirs. These reservoirs show a better-than-expected primary performance: lower production gas/oil ratios (GORs), higher-than-expected production rates, and higher oil recovery. A mechanism used to account for the observed performance is that the liberated solution gas is entrained in the oil when the reservoir pressure falls below the thermodynamic equilibrium bubblepoint pressure. The presence of entrained gas increases the effective compressibility of the oil phase and prevents gas from becoming a free phase. Hence, the foamy oil behaves as if it had a pseudobubblepoint pressure below the usual equilibrium bubblepoint pressure. This paper describes a pseudobubblepoint model and a methodology that can be used to compute foamy-oil fluid properties from conventional laboratory pressure/volume/temperature (PVT) data. The techniques developed are then used to study foamy oil in the Orinoco belt, Venezuela. The present mathematical model is validated by comparing numerical and experimental results.

Introduction

Conventional oils, as limited resources, have been exhausted daily. It is difficult for these resources to close the gap with oil requirements from economic growth that has peaked oil price as high as USD115/bbl. Additional development will be primarily in the form of unconventional resources that consist of low-permeability-oil (tight oil), shale-oil, heavy-oil, and oil-sands reserves.

More than 6 trillion bbl (1 trillion m^3) of oil in place are attributed to the heaviest hydrocarbons—triple the combined world reserves of conventional oil and gas. Natural crude oils usually exhibit a continuum of densities and viscosities. Viscosity of heavy oil at reservoir temperature is often the most important measure to an oil producer because it determines how easily oil flows. Density is also important to an oil refiner because it is a better indicator of the yield from distillation. Unfortunately, no clear correlation exists between the two. Medium-density or light crude with high paraffin content in a shallow cool reservoir can have a higher viscosity than heavy, paraffin-free crude in a deep hot reservoir. Viscosity varies greatly with temperature, whereas density varies little. Density has become the more commonly used oilfield standard for categorizing crude oils.

Density is usually defined in terms of American Petroleum Institute (API) gravity, which is related to specific gravity (SG)—the denser the oil, the lower the API gravity (Conaway 1999). Liquid-hydrocarbon gravities range from 4°API for tar-rich bitumen to 70°API for condensates. Heavy oil occupies a range along this continuum between ultraheavy oil and light oil. Heavy oil is defined as gravities between 10°API and 20.0°API at reservoir conditions (Nehring et al. 1983; Chen 2006). However, nature does not recognize such boundaries. In some reservoirs, oil with gravity as low as 7°API or 8°API is still considered heavy rather than ultraheavy because one can extract it by heavy-oil production methods.

In this paper, we focus on reservoirs with oils of gravities between approximately 10°API and 20°API and the technologies used to develop them. As an indication of the problems that arise, the most-viscous tar, pitch, and bitumen deposits at even lower API gravities often require mining-style techniques or steam-related recovery processes for economic exploitation.

When originally generated by petroleum source rock, crude oil is not heavy. Almost all crude oils originate with gravity between 30°API and 40°API; oil becomes heavy only after substantial degradation during migration and after entrapment (Curtis et al. 2002). Degradation involves a variety of biological, physical, and chemical processes. Bacteria borne by surface water metabolize paraffinic, aromatic, and naphthenic hydrocarbons into heavier molecules (Tissot and Welte 1978). Formation water also removes hydrocarbons through solution, washing away lighter molecular hydrocarbons that are more soluble in water. In addition, crude oil degrades by devolatilization when a poor-quality seal allows lighter molecules to separate and escape.

Heavy oils are typically produced from geologically young reservoirs: Pleistocene, Pliocene, and Miocene. These reservoirs are shallow and have less-effective seals, thus exposing them to conditions conducive to forming heavy oils. The shallow nature of most heavy-oil reservoirs means that many were discovered as soon as human beings settled nearby. Collecting oil from seeps and digging by hand were the earliest and most primitive means of recovery, followed by mining and tunneling.

In the early 1900s, these primitive techniques were replaced by techniques some of which are still used today to produce heavy oils. Most practitioners try to produce as much oil as possible under primary recovery, termed "cold production," at reservoir temperature. Typical recovery factors (percentage of the oil in a reservoir that can be recovered) by cold production range from 1 to 10%. Depending on oil properties, primary production with artificial lift, including injection of a light oil or diluents to reduce viscosity, can be very effective.

Many fields produce most efficiently with horizontal production wells. In some cases, using foamy-oil behavior and/or encouraging sand production along with oil is a preferred production strategy. Choosing the optimal cold-production strategy requires an understanding of rock and fluid properties.

The fraction of original oil in place (OIP) (OOIP) that one can recover by solution-gas drive decreases with increasing oil viscosity. For heavy-oil reservoirs, the expected recovery factor by solution-gas drive is typically approximately 5% (Tang et al. 2006). However, a number of heavy-oil reservoirs under solution-gas drive show anomalous primary performance: low production GORs, high oil-production rates, and high oil recovery. A couple of mechanisms were identified as the cause of this unusual production behavior. The first production mechanism, called "foamy oil," is gas-bubble expansion, which gives the oil a foamy feature because bubbles are trapped by the oil, and recovery is enhanced by solution-gas drive. Ultimate oil recovery can be as high as 20% in the primary performance of some heavy-foamy-oil reservoirs (Wang et al. 2008). The second production mechanism is the internal erosion in unconsolidated-sand reservoirs that can create a network of high-permeability channels, termed "wormholes." This

Original SPE manuscript received for review 30 May 2012. Revised manuscript received for review 25 April 2014. Paper (SPE 172345) peer approved 29 May 2014.

mechanism can enhance the drainage by a factor of 10 or more, but it involves complex sand production. Wormhole formation and localization are not completely understood; thus, it is difficult to optimize production (Tremblay 2005; Chen 2006). In this paper, we concentrate on foamy-oil flow in heavy-oil reservoirs. A third paper of this series will study wormhole formation and transport.

In all solution-gas-drive reservoirs, gas is released from solution as the reservoir pressure declines. Gas initially exists in the form of small bubbles created within individual pores. As time evolves and pressure continues to decline, these bubbles grow to occupy the pores. With a further decline in pressure, the bubbles created in different locations become large enough to coalesce into a continuous gas phase. Conventional wisdom indicates that the discrete bubbles that are larger than pore throats remain immobile (trapped by capillary forces) and gas flows only after the bubbles have coalesced into a continuous gas phase. After the gas phase becomes continuous [which is equivalent to the gas saturation becoming larger than critical, the minimal saturation at which a continuous gas phase exists in porous media (Chen et al. 2006)], traditional two-phase (gas and oil) flow with classical relative permeabilities occurs. A result of this evolution process is that the production GOR increases rapidly after the critical gas saturation has been exceeded.

Field observations in some heavy-oil reservoirs, however, do not fit into this solution-gas-drive description in that the production GOR remains relatively low. The recovery factors in such reservoirs are also unexpectedly high. A simple explanation of these observations could be that the critical gas saturation is high in these reservoirs. This explanation cannot be confirmed by direct laboratory measurement of the critical gas saturation. An alternative explanation of the observed GOR behavior is that gas, instead of flowing only as a continuous phase, also flows in the form of a gas-in-oil dispersion. This type of dispersed gas/oil flow is what is referred to as "foamy-oil flow."

Although the unusual production behavior in some heavy-oil reservoirs was observed as early as the late 1960s, Smith (1988) appears to have been the first to report it, and he used the terms "oil/gas combination" and "mixed fluid" to describe the mixture of oil and gas that is entrained in heavy oil as very tiny bubbles. Baibakov and Garushev (1989) used the term "viscous-elastic system" to describe highly viscous oil with very fine bubbles present. Sarma and Maini (1992) were the first to use the phrase "foamy oil" to describe viscous oil that contains dispersed gas bubbles. Claridge and Prats (1995) used the terms "foamy heavy oil" and "foamy crude." Although there is continuing debate on the suitability of the term "foamy-oil flow" to describe the anomalous flow of the oil/gas mixture in the primary production of heavy oil, this expression has become a fixture in the petroleum-engineering terminology (Maini 1996). Finally, we mention that the concept of a higher critical gas saturation was used in Treinen et al. (1997) for solution-gas drive in a heavy-oil reservoir.

The actual structure of foamy-oil flow and its mathematical description are still not well-understood. Much of the earlier discussion of such flow was based on the concept of microbubbles [i.e., bubbles much smaller than the average pore-throat size and thus free to move with the oil during flow (Sheng et al. 1999a)]. One can produce this type of dispersion only by the nucleation of a very large number of bubbles (explosive nucleation) and by the presence of a mechanism that prevents these bubbles from growing into larger bubbles with decline in pressure (Maini 1996). This hypothesis has not been supported by experimental evidence.

A more-plausible hypothesis on the structure of foamy-oil flow is that it involves much larger bubbles migrating with the oil and that the dispersion is created by the breakup of bubbles as a result of capillary trapping and viscous mobilizing forces during their migration with the oil. The major difference between the conventional solution-gas drive and the foamy-solution-gas drive is that the pressure gradient in the latter is strong enough to mobilize gas clusters after they have grown to a certain size. Maini (1996) presented experimental evidence that supports this hypothesis for foamy-oil flow. This hypothesis seems consistent with the visual observations in micromodels that show the bubble size to be larger than the pore size. The mechanism for foamy-oil behavior remains to be fully understood. The objective of this paper and its previous companion paper, Wang et al. (2008), is to study foamy-oil behavior through experimental, mathematical, and numerical means.

The paper is organized as follows. In the next section, we review the foamy-oil models available in the literature. In the third section, we develop a pseudobubblepoint model. In the fourth section, we validate this model by comparing experimental and simulation results. In addition to the use of the experimental results from our previous companion paper, Wang et al. (2008), the experimental results from Bennion et al. (2003) are used to validate the developed model further. In the last section, we give concluding remarks.

State of the Art of Foamy-Oil Models

To date, a mathematical model of foamy solution-gas drive that incorporates the physics of generation and the flow of gas-in-oil dispersion is not available. The numerical simulation of the primary production of foamy-oil reservoirs has so far used empirical adjustments to conventional solution-gas-drive models to account for the presence of dispersed flow. Various solution-gas-drive models related to foamy-oil flow and their limitations are briefly reviewed.

The most-straightforward approach to model foamy-oil flow is to adjust process parameters in conventional solution-gas-drive models. A history match of reservoir performance is obtained with existing simulators by adjusting some parameters to account for the contributions of foamy-oil flow to oil recovery. These parameters include the absolute permeability, oil and gas relative permeabilities, fluid and rock compressibilities, critical gas saturation, and oil viscosity (Loughhead and Saltuklaroglu 1992). The conventional models cannot capture the peculiar features of dispersed flow such as the dynamic processes involved in the generation and collapse of dispersion.

The earliest model for a heavy-oil reservoir involving two-phase flow with gas in the form of tiny bubbles moving with oil was proposed by Smith (1988). Under the assumption that the compressibility of the mixture of heavy oil and gas bubbles is $c_f = \kappa/p$, where κ is an empirical constant and p is the mixture pressure, a solution-gas-drive model was obtained to define the peculiar pressure-dependent multiphase-flow properties and to describe the flow of the mixture. According to this model, the amount of gas entrained in the oil depends on the constant κ and the pressure p but is independent of time and flow conditions.

Modified fractional-flow models attempt to match the production behavior by modifying fractional-flow curves obtained from the gas and oil relative permeabilities. Lebel (1994) developed a model that assumes that all released solution gas remains entrained in the oil phase up to a certain system-dependent limiting volume fraction. As a result, as the gas saturation increases from zero, the fractional flow of gas increases linearly with saturation until the limiting entrained gas saturation is reached. Beyond the limiting volume fraction of gas in the foamy oil, any further increase in the gas saturation will lead to free gas. The effective viscosity of foamy oil decreases slightly from that of oil as the volume fraction of gas increases, and the density of the foamy oil is a volume-weighted average of the densities of oil and gas. An equilibrium gas/oil PVT relationship was exploited in this model. The fractional-flow curve was calibrated to match laboratory data during the blowdown of "live" oil in laboratory cores. Finding a correct fractional-flow curve requires trial and error. Modified fractional-flow models capture a feature of foamy-oil flow—some fraction of evolved gas is entrained in oil. However, relating the effective viscosity of the foamy oil to the volume fraction of gas is quite difficult.

Claridge and Prats (1995) described a model for simulating the anomalous foamy-oil production behavior. They indicated that the asphaltenes present in the crude oil adhere to gas bubbles when the latter are still tiny. This coating of asphaltenes on the bubble surfaces stabilizes the bubbles at a small size. The bubbles

continue to flow through the rock pores with the oil. This model differs from the others mentioned previously in the description of the net effect of asphaltene adsorption onto the bubble surfaces on the viscosity of the crude oil. They suggested that the oil viscosity decreases dramatically because of the removal of the dispersed asphaltenes. It is difficult to see why the transfer of asphaltenes to bubble surfaces would have a large effect on the dispersion viscosity because the asphaltenes adsorbed on the bubble surfaces are still a part of the dispersed phase.

Recently, Sheng et al. (1999b) described dynamic-flow models that involve two rate processes: a rate process that controls the transfer from solution gas to evolved gas and a process that controls the transfer rate from evolved gas to free gas. Two phases (foamy oil and gas) are modeled by use of the conventional two-phase relative permeabilities. The dispersed gas is assumed to flow with the oil as if it were a part of the liquid phase that has the compressibility and density of the gas phase but a viscosity equal to the liquid-oil viscosity. Bubble growth is described by an exponential growth function (an empirical correlation), and the disengagement of dispersed gas bubbles from the oil is assumed to decay exponentially also.

Dynamic-flow models account for time-dependent changes in the dispersion characteristics using simple rate processes. They represent a greater improvement than the other models discussed previously. However, the rate processes involved in foamy solution-gas drive seem to be controlled by the rock/fluid properties and the capillary number. Thus, the rate constants inferred by history matching a known-depletion reservoir are not valid for predicting the outcome of a new reservoir involving different flow properties.

Joseph et al. (2002) presented a mathematical model that depends only on the velocity through Darcy's law, the pressure, and the dispersed gas fraction. This model governs only in scenarios in which bubbles do not coalesce to generate the percolation of free gas. In their theory, the bubbles move with the oil as they evolve. The primary empirical content of the theory enters through the derivation of solubility isotherms that one can obtain from PVT data. The modeling of nucleation, coalescence, bubble drag laws, and transfer functions is avoided. The local pressure difference and dispersed gas fraction are in equilibrium on the solubility isotherms. In a pressure drawdown, the time taken for the system to return to equilibrium is given by a rate law characterized by an empirical relaxation time (rate constant). The virtue of the model is simplicity, but it works only for relatively immobile dispersed gas bubbles in which divergence-free velocities (zero divergence) are excluded. This model cannot be expected to give rise to a percolation threshold or even to a critical gas fraction.

In summary, a simulation model capable of predicting the performance of foamy-oil reservoirs under different operating conditions is unavailable. It is the aim of this paper to develop a mathematical model on the basis of the pseudobubblepoint-pressure concept from our experimental study (Wang et al. 2008). This concept is suitable for simulation studies because the pseudobubblepoint pressure can be tuned for different cases to capture the foamy-oil PVT data for a corresponding production process.

A Pseudobubblepoint Model

Kraus et al. (1993) were the first to present the pseudobubblepoint concept for primary depletion in foamy-oil reservoirs. The pseudobubblepoint pressure in this concept is an adjustable parameter in the fluid-property description, and all the released solution gas remains entrained in the oil until the reservoir pressure drops to this pseudobubblepoint pressure. Below this pressure, only a fraction of the released gas remains entrained, and the gas fraction decreases linearly to zero with declining pressures. The dispersed gas is treated as a part of the oil phase, but its molar volume and compressibility are calculated with those of the free gas. According to the amount of the gas dispersed in the oil phase, the compressibility of foamy oil is evaluated as a function of pressure, and then this enhanced compressibility is substituted for that of the dead-oil component in the conventional commercial Scientific Software-Intercomp, Inc. thermal simulator. Although the pseudobubblepoint concept was used, a mathematical model that is based on this concept has not been derived.

Mastmann et al. (2001) also used the pseudobubblepoint concept to predict foamy-oil behavior. The commercial black-oil simulator Eclipse was used in their numerical simulation. The model equations at the foundations of this simulator are based on the conventional multiphase flow in the setting of classical relative permeabilities, which is not suited to the description of a fluid mixture in which the oil and dispersed gas move in the same phase.

From our recent laboratory experiments for foamy oil (Wang et al. 2008), we have seen that the pseudobubblepoint concept can capture important features present in foamy-oil flow and can predict the anomalous production behavior of foamy-oil reservoirs. We will develop a realistic model with this concept. The assumptions on which our model is based are

- Foamy oil is assumed to consist of three chemical components: (a) dead oil; (b) solution gas that has the viscosity, compressibility, and molar density of the normal solution gas; and (c) dispersed gas that has the compressibility and density of the gas phase but a viscosity equal to the liquid-oil viscosity (i.e., dispersed gas bubbles are assumed to flow with the oil as if they were part of the liquid phase).
- The gas phase is assumed to contain only the free-gas component.
- Microbubbles are dispersed in the liquid-oil phase, and the capillary pressure on the surface of a bubble is related to the bubble size. Because the bubble size is not considered in the present model, the capillary pressure on the bubble surface is ignored.
- Darcy's laws are assumed to hold for both the foamy-oil and gas phases.
- It is known that diffusion does not affect dispersion significantly in the case of large scales. Thus, the diffusion of an oil or gas component that is caused by its concentration difference is omitted.
- The basic mechanism of foamy-oil behavior is related to the existence of a pseudobubblepoint in the reservoir under consideration.

Mass-Balance Equations. Let ϕ be the porosity of the reservoir, and S_{fo}, ρ_{fo}, u_{fo}, and q_{fo} be the saturation, mass density, volumetric velocity, and volumetric rate of the foamy-oil phase, respectively. Similarly, let S_g, ρ_g, u_g, and q_g be the corresponding quantities of the gas phase. Also, letρ_{fo}^{do}, ρ_{fo}^{sg}, and ρ_{fo}^{dg} be the partial mass densities of the dead-oil, solution-gas, and dispersed-gas components in the foamy-oil phase, respectively. The material-balance equation for the dead-oil component in the foamy oil phase is

$$\frac{\partial(\phi S_{fo}\rho_{fo}^{do})}{\partial t}+\nabla\cdot(\rho_{fo}^{do}u_{fo})=q_{fo}, \quad \ldots\ldots\ldots\ldots\ldots (1)$$

and for the overall-gas component, it is

$$\frac{\partial\{\phi[S_{fo}(\rho_{fo}^{sg}+\rho_{fo}^{dg})+S_g\rho_g]\}}{\partial t}+\nabla\cdot[(\rho_{fo}^{sg}+\rho_{fo}^{dg})u_{fo}+\rho_g u_g]=q_g. \quad \ldots\ldots\ldots\ldots\ldots (2)$$

Darcy's Law. Darcy's law is assumed to hold for the foamy-oil phase,

$$u_{fo}=-\frac{k_{rfo}}{\mu_{fo}}k(\nabla p_{fo}-\rho_{fo}\wp\nabla z), \quad \ldots\ldots\ldots\ldots\ldots (3)$$

and for the gas phase,

$$u_g=-\frac{k_{rg}}{\mu_g}k(\nabla p_g-\rho_g\wp\nabla z), \quad \ldots\ldots\ldots\ldots\ldots (4)$$

where k is the permeability of the reservoir; μ_α, $k_{r\alpha}$, and p_α are, respectively, the viscosity, relative permeability, and pressure of the α phase, $\alpha = fo, g$; $\wp$ is the magnitude of the gravitational acceleration; and z is the depth.

TABLE 1—DEPLETION PVT TEST RESULTS (MASTMANN ET AL. 2001; TREMBLAY 2005)

Pressure (psig)	GOR ($stdm^3/m^3$)	B_o	Viscosity (cp)	Density (g/cm^3)
2,524	31.17	1.0697	1,195	0.9719
2,300	31.17	1.0727	900	0.9692
2,150	31.17	1.1297	876	0.9203
2,000	31.17	1.1437	974	0.9090
1,850	30.89	1.1467	1,067	0.9064
1,700	28.79	1.1411	1,182	0.9091
1,550	26.08	1.1134	1,399	0.9298
1,400	24.24	1.0857	1,582	0.9518
1,250	21.99	1.0695	1,847	0.9653
1,100	20.05	1.0625	2,173	0.9705
900	17.76	1.0539	2,614	0.9770
700	14.81	1.0447	3,087	0.9846
500	12.05	1.0367	3,690	0.9897
300	8.27	1.0280	4,286	0.9969
200	6.24	1.0238	4,692	0.9990
100	3.49	1.0213	5,655	0.9997
50	2.11	1.0193	6,800	1.0007
0	0	1.0180	8,129	1.0006

Additional Constraints. Two phases (foamy oil and gas) coexist in the reservoir. Their saturations satisfy the constraint

$$S_{fo} + S_g = 1. \quad \ldots\ldots\ldots\ldots\ldots\ldots\ldots\ldots\ldots\ldots \quad (5)$$

There are three components in the liquid foamy-oil phase: dead oil, solution gas, and dispersed gas. The mass density of this phase is given by the partial densities:

$$\rho_{fo} = \rho_{fo}^{do} + \rho_{fo}^{sg} + \rho_{fo}^{dg}. \quad \ldots\ldots\ldots\ldots\ldots\ldots\ldots\ldots\ldots\ldots \quad (6)$$

The phase pressures are related by capillary pressures:

$$p_{cgfo} = p_g - p_{fo}. \quad \ldots\ldots\ldots\ldots\ldots\ldots\ldots\ldots\ldots\ldots \quad (7)$$

Fluid Properties. For foamy oil, because of the high viscosity of the oil, the gas bubbles cannot immediately coalesce together to form bubbles large enough to allow gravitational forces to separate gas from the oil. For this reason, the oil phase remains as a continuous dispersed gas/oil emulsion with a higher concentration of increasingly larger bubbles trapped in a milkshake-like format within the oil as the reservoir pressure declines, as discussed earlier. The point for the foamy oil at which the bubbles of free gas can finally begin to separate from solution as a distinct free-gas phase is referred to as the pseudobubblepoint.

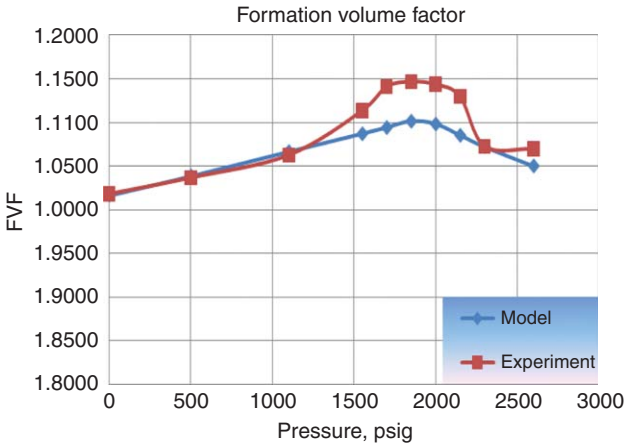

Fig. 1—Experimental and calculated FVFs.

We focus on the study of the formation volume factor (FVF) B_{fo}, density ρ_{fo}, viscosity μ_{fo} for the foamy oil and the solution GOR, which play a dominant role in determining the performance of oil recovery. For the sake of interest, typical experimental results for these data are shown in **Table 1** (Treinen et al. 1997; Mastmann et al. 2001) and illustrated in **Figs. 1–4,** which also include the calculated data (see next).

FVF. The FVF is one of the properties affected most by foamy oil and may be one of the major contributions to the cause of the anomalous production behavior. Conventional oil shrinks below the true bubblepoint because of the evolution of gas from the oil, whereas the foamy oil can quickly expand between this point and the pseudobubblepoint. The reason is that highly compressible gas is freed from solution, but remains trapped in the oil phase. Hence, there is a mechanism that accounts for the high apparent compressibility of the flowing fluid. Because the free-gas phase is retarded, the foamy oil is the only phase that can be mobilized from reservoirs until the pseudobubblepoint pressure is reached and then free gas is evolved from the oil.

The FVF for the foamy oil, B_{fo}, is defined as the ratio of the volume of dead oil plus its dissolved gas and dispersed gas (measured at reservoir conditions) to the volume of the oil component at standard conditions:

$$B_{fo} = \frac{V_{do} + V_{dg} + V_{sg}}{V_{doS}}, \quad \ldots\ldots\ldots\ldots\ldots\ldots\ldots\ldots\ldots\ldots \quad (8)$$

where S stands for the standard conditions. In practical simulation, one can calculate B_{fo} as follows (Standing 1981):

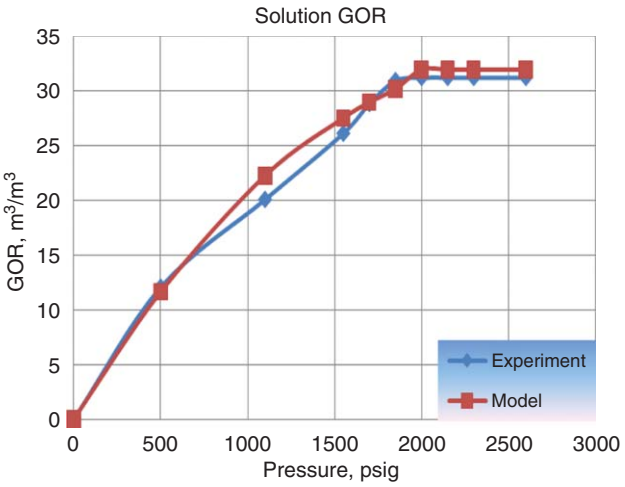

Fig. 2—Experimental and calculated GORs.

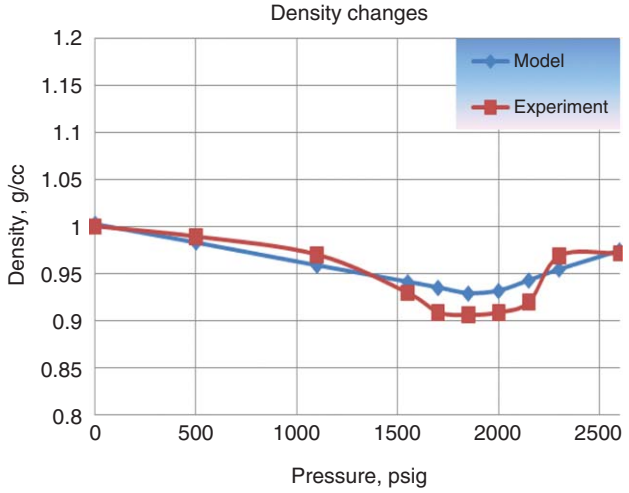

Fig. 3—Calculated entrained-gas-volume fraction.

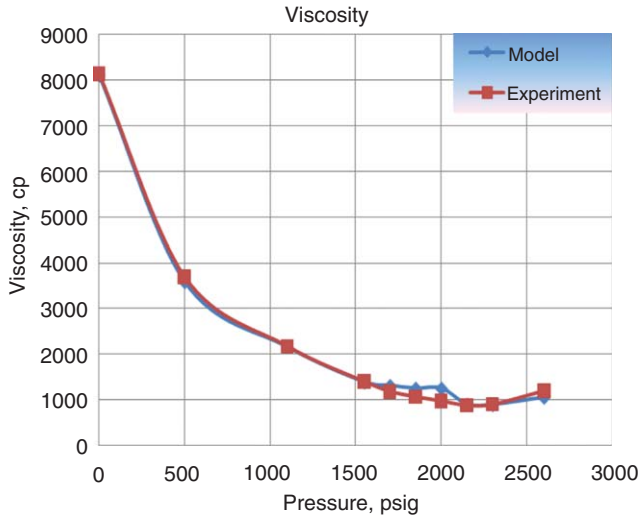

Fig. 4—Experimental and calculated densities.

$$B_{fo} = \frac{62.4\gamma_{foS} + 0.0136R_{so}\gamma_{gS}}{\rho_{fo}},$$

where R_{so} is the GOR and γ_{foS} and γ_{gS} are the specific gravities of the foamy oil and gas at stock-tank conditions, respectively. A typical B_{fo} is illustrated in Fig. 1.

The FVF for gas, B_g, is the ratio of the volume of the gas phase measured at reservoir conditions to the volume of the gas component measured at standard conditions:

$$B_g(p,T) = \frac{V_g(p,T)}{V_{gS}}. \quad \ldots\ldots\ldots\ldots\ldots\ldots\ldots\ldots\ldots\ldots \quad (9)$$

GOR. For conventional oil, the GOR decreases after the true bubblepoint is reached. Foamy oil, however, results in a situation in which this GOR remains constant until the pseudobubblepoint is reached. This phenomenon must be incorporated into the mathematical modeling.

The GOR, R_{so}, is the volume of solution gas (measured at standard conditions) dissolved at a given pressure and reservoir temperature in a unit volume of stock-tank oil:

$$R_{so}(p,T) = \frac{V_{sgS}}{V_{doS}}. \quad \ldots\ldots\ldots\ldots\ldots\ldots\ldots\ldots\ldots\ldots \quad (10)$$

In practice, one can directly calculate R_{so} (Treinen et al. 1997; Mastmann et al. 2001):

$$R_{so} = \begin{cases} R_{bs}, & p_{pb} \le p \le p_b \\ R_s + \alpha_g(R_{bs} - R_s), & p_{\text{ref}} \le p \le p_{pb} \end{cases},$$

where p_b is the true bubblepoint pressure, p_{pb} is the pseudobubblepoint pressure, R_{bs} is the GOR at p_{pb}, R_s is the conventional GOR at any pressure, α_g is the fraction of gas dispersed in the oil phase, and p_{ref} is a reference pressure (lower than p_{pb}). As previously noted, all the released solution gas remains entrained in the oil until the reservoir pressure drops to p_{pb}. Below this pressure, only a fraction of the released gas remains entrained, and the gas fraction can linearly decrease to zero as pressure declines to the reference pressure p_{ref}. In this case, the entrained-gas fraction α_g is defined as

$$\alpha_g(p) = \begin{cases} 1, & p_{pb} \le p, \\ \dfrac{p - p_{\text{ref}}}{p_{pb} - p_{\text{ref}}}, & p_{\text{ref}} \le p \le p_{pb}, \\ 0, & p \le p_{\text{ref}}. \end{cases}$$

Typical functions for R_{so} and α_g are demonstrated in Figs. 2 and 3, respectively.

Densities. The density of foamy oil behaves in a manner opposite to that of the FVF. Below the true bubblepoint, the density of conventional oil increases because of the evolution of gas from the oil phase. However, the foamy-oil density declines, caused by the entrapping of gas bubbles in the oil, as pressure decreases.

The mass densities at reservoir conditions are related to the densities at standard conditions by

$$\rho_{fo}^{do}(p,p_b) = \frac{\rho_{foS}}{B_{fo}(p,p_b)},\ \rho_{fo}^{sg}(p,p_b) = \frac{\rho_{gS}R_{so}}{B_{fo}(p,p_b)},\ \rho_g(p,p_b) = \frac{\rho_{gS}}{B_g(p)}, \quad \ldots\ldots\ldots\ldots\ldots\ldots\ldots\ldots \quad (11)$$

where the second equation describes the mass density of solution gas in the foamy oil. For the reservoir pressure between the true and pseudobubblepoint pressures, opposite to the entrained-gas fraction α_g, we define the "saturation" of the dispersed gas by

$$S_{fo}^{dg}(p,p_b) = \frac{V_g}{V_{dg}}. \quad \ldots\ldots\ldots\ldots\ldots\ldots\ldots\ldots\ldots\ldots \quad (12)$$

By use of the third equation of Eq. 11, we see that

$$S_{fo}^{dg}(p,p_b) = \frac{\rho_{fo}^{dg}}{\rho_g} = \frac{\rho_{fo}^{dg}B_g}{\rho_{gS}},$$

so that the partial density of the dispersed gas is

$$\rho_{fo}^{dg} = \frac{S_{fo}^{dg}\rho_{gS}}{B_g}. \quad \ldots\ldots\ldots\ldots\ldots\ldots\ldots\ldots\ldots\ldots \quad (13)$$

An alternative approach to define the foamy-oil density is given as follows: If we group the dead oil and dispersed gas as a mixture (lumping), we can evaluate the density of this mixture as (Standing 1981)

$$\rho_o = \frac{62.4\gamma_{oS} + 0.0136R_s\gamma_{gS}}{0.972 + 0.000147\left[R_s\left(\dfrac{\gamma_{gS}}{\gamma_{oS}}\right) + 1.25(T - 460)\right]^{1.175}},$$

where γ_{oS} is the SG of stock-tank oil. Now, we can compute the foamy-oil density by (Kumar and Mahadevan 2008)

$$\rho_{fo} = \rho_o(1 - \beta) + \rho_g\beta,$$

where the variable β represents the volume fraction of gas entrained in the foamy-oil phase,

$$\beta = \frac{\alpha_g\phi_g}{1 - \phi_g(1 - \alpha_g)},$$

and ϕ_g is the ratio of the volume of gas flashed into the volume of the total solution gas. A typical ρ_{fo} by means of this approach is shown in Fig. 4.

Viscosities. The treatment of the apparent viscosity of foamy oil between the true bubblepoint and the pseudobubblepoint requires special care. Below the true bubblepoint, the viscosity of conventional oil increases because gas freely evolves from the oil. For foamy oil, conventional wisdom is that its viscosity should remain relatively constant, or may decrease slightly between the two bubblepoints. However, it is well-known that gas/liquid rheology often results in an increase in viscosity. Experiments need to be conducted to understand how the extreme viscosity of the base fluid phase for foamy oil interacts with gas and how it depends on the flow conditions, which will be a future task of this group.

Empirical formulas for the foamy-oil viscosity can be given as follows. Below the pseudobubblepoint, it is

$$\mu_{fo} = \mu_o\exp[m_1(R_s - R_{so})],$$

where μ_o is the conventional oil viscosity and m_1 is an empirical constant. Above the pseudobubblepoint, it is related to the large bubble size and the intention of nucleation to the continuous gas (i.e., the intention of bubbles to coalesce to larger bubbles in the continuous gas) but to still remain entrained in the oil phase:

$$\mu_{fo} = \mu_o(p)\exp[m_2(p - p_0)],$$

where p_0 is the initial reservoir pressure and m_2 is an empirical constant.

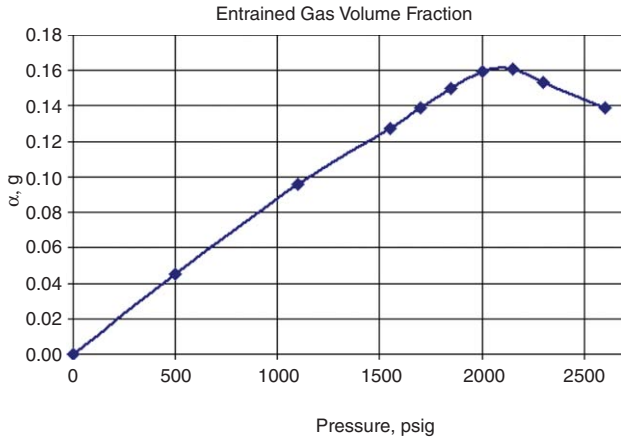

Fig. 5—Experimental and calculated viscosities.

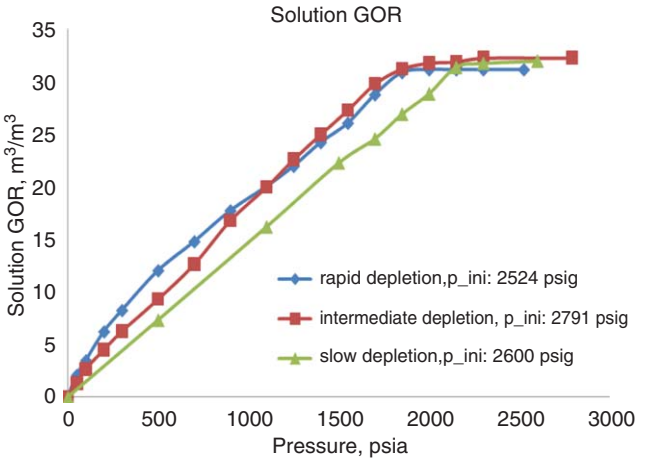

Fig. 6—Solution GOR profiles vs. different depletion rates.

A typical μ_{fo} is given in **Fig. 5.** All the calculated PVT data in Figs. 1 through 5 match the experimental results very well.

Other Properties. Foamy-oil behavior is strongly related to depletion rates. A rapid decline in pressure allows little time for gas bubbles to nucleate and promotes more foaming. Slow depletion rates allow more time for gravitational and IFT forces to coalesce the gas bubbles and for gradual evolution to occur. Because varying depletion rates occur in different locations of a reservoir, one can conduct experiments with a number of rates to see their effect on foamy-oil behavior. Here, the solution GORs vs. different depletion rates are shown in **Fig. 6.** This shows that the solution GOR decreases as the rate decreases.

For foamy-oil reservoirs, the effect of relative permeabilities on recovery factors appears more pronounced than for conventional oil reservoirs. To date, directly measured solution-gas-drive relative permeabilities are not available. Conventional relative permeability data were used. A major focus of future experiments will be the acquisition of relative permeability data for foamy oil. The relative permeabilities can depend on the flow conditions and the flow history.

Numerical-Simulation Results

For the numerical solution of the foamy-oil model by means of a code that we developed, the choice of the primary unknowns depends on the states. When the reservoir pressure is above the true bubblepoint pressures, the unknowns are (p_{fo}, p_b), following the traditional black-oil-model approach (Chen et al. 2006). For the reservoir pressure between the true and pseudobubblepoint pressures, they are (p_{fo}, S_{fo}^{dg}). Finally, when reservoir pressure is below the pseudobubblepoint pressure, they are (p_{fo}, S_g). The history-matching process in the following two cases is performed by adjusting the relative permeability curves and a suite of reaction factors that describe the transition process for gas dispersion. Above the pseudobubblepoint, the reaction rate was approximately 0.002; below it, this rate is approximately 0.005. One of the examples for the relative permeability data is given in **Table 2.**

TABLE 2—RELATIVE PERMEABILITIES

S_g	k_{rg}	k_{rfo}
0	0	1
0.001	0	1
0.02	0	0.997
0.05	0.005	0.98
0.12	0.025	0.7
0.2	0.075	0.35
0.25	0.125	0.2
0.3	0.19	0.09
0.4	0.41	0.021
0.45	0.6	0.01
0.5	0.72	0.001
0.6	0.87	0.0001
0.7	0.94	0
0.85	0.98	0
1	1	0

Case Study I. The objective of this case study is to validate the developed model with drainage experiments with Orinoco-belt heavy oil in a long laboratory core in simulated reservoir conditions (Wang et al. 2008). The reservoir properties used in simulation are listed in **Table 3,** and the foamy-oil PVT table is shown in **Table 4.** The rock permeability is kept constant during the simulation to be consistent with the laboratory experiments.

A full 3D model is applied to simulate the depletion experiments. A finite-volume method is used to discretize this model, and a grid consisting of 12 blocks along the x-axis and seven gridblocks along both the y-axis and z-axis (a uniform grid) is used. The size of each gridblock is $100 \times 100 \times 10$ ft. A maximal timestep size of 50 days and a minimal timestep size of 1 day are specified. The simulation runs are under bottomhole-pressure control, the initial pressure is 1,700 psi to be consistent with the experimental setup, and the external boundary condition is of a no-flow type. The recovery factor and production GOR are

TABLE 3—RESERVOIR PROPERTIES FOR FIELD-SCALE SIMULATION

Reservoir length	2,500 ft
Reservoir width	2,500 ft
Reservoir thickness	15 ft
Initial pressure	1,750 psi
Bubblepoint pressure	1,230 psi
Pseudobubblepoint pressure	700 psi
Initial permeability	500 md
Initial porosity	30%
Oil viscosity	1,195 cp
Density of oil	49.1 lbm/ft^3
Density of gas	0.06054 lbm/ft^3
Density of water	64.79 lbm/ft^3
Bottomhole pressure	1,000 psi
Cartesian grid size	$50\times50\times3$ (x, y, z)
Initial water saturation	0.311
Initial oil saturation	0.689
Water compressibility	3.0×10^{-7} psi^{-1}
Formation compressibility	4.0×10^{-5} psi^{-1}

TABLE 4—FOAMY-OIL PVT DATA			
P (psia)	Bo (m^3/m^3)	Viscosity (cp)	SolGOR (m^3/m^3)
14.7	1.0361	7433	0
314.7	1.1021	4102	21.204
414.7	1.1236	3499	27.942
614.7	1.1633	2790	41.417
814.7	1.2052	2328	54.893
1014.7	1.2072	2214	68.368
1214.7	1.1091	1649	81.844
1414.7	1.0977	1774	88.153
1614.7	1.0808	1900	89.276

calculated. **Figs. 7 and 8,** respectively, indicate the profiles of these two variables with pressure depletion. Generally, one can determine the bubblepoint pressure and pseudobubblepoint pressure (approximately 700 psi) from these two curves according to the different phases of production. Rock-and-fluid expansion starts the depletion. Note that the reservoirs under foamy-oil solution-gas drive are produced with unconsolidated formation. The unconsolidated formation also results in a higher compressibility, which can yield higher-than-usual recovery.

After the initial stage, the production is under way between the true bubblepoint pressure and the pseudobubblepoint pressure. During this period, three reactions coexist (i.e., gas dispersion, bubble nucleation, and free-gas evolution). The oil with dispersed bubbles provides tremendous energy to the formation to maintain a relatively high oil-production rate. Fig. 8 indicates a steep increase in oil recovery, which suggests the effect of foamy solution-gas drive on oil recovery.

Below the pseudobubblepoint pressure, both dispersed bubbles and dissolved gas develop into a continuous gas phase. Because of greater mobility, it results in gas breakthrough and a big jump in production GOR. Correspondingly, oil recovery experiences a further increase. From these two curves, one can see that the pattern of the experimental and simulation results matches well. Although a relatively coarse grid is used here, finer grids indicate a similar pattern match.

Case Study II. To further validate the developed foamy-oil model, the Patos-Marinza Driza heavy-oil core tests on primary depletion (Bennion et al. 2003) are used. The core plug and fluid properties are shown in **Tables 5 and 6** (Maini 1999; Mastmann et al. 2001). The pseudobubblepoint pressure was approximately 1,200 psi.

To be consistent with the experimental tests in Bennion et al. (2003), a 1D model is applied to simulate the depletion experiments, and it consists of three gridblocks along the x-axis to simulate a 15-cm-long core plug. A uniform gridblock size of 5 cm is used. The simulation proceeds with an initial pressure of 3,300 psi. A timestep size of 120 seconds is used. The information at the preceding timestep is used to estimate the fluid properties at the present timestep.

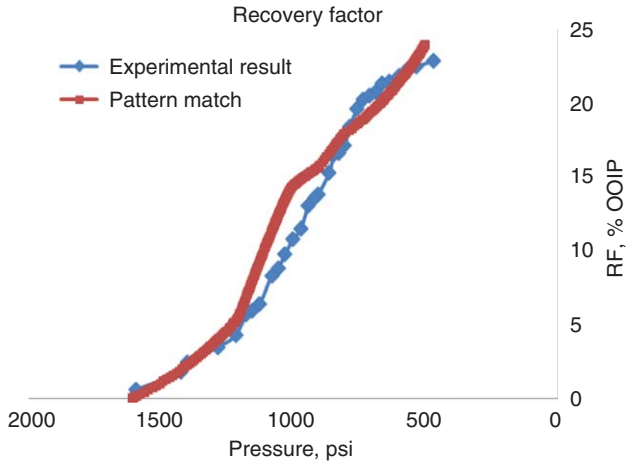

Fig. 8—Recovery factor, experimental vs. simulation results.

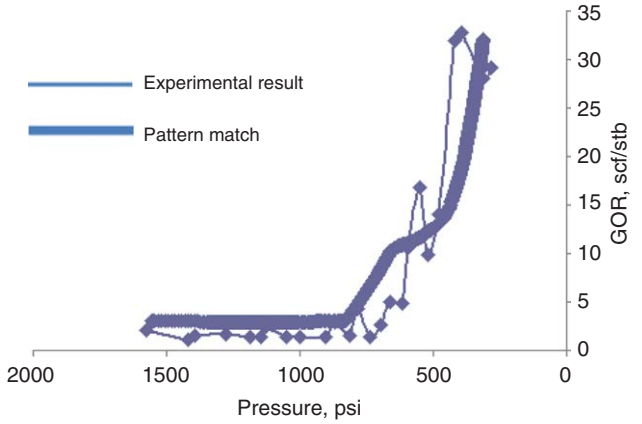

Fig. 7—Production GOR, experimental vs. simulation results.

Figs. 9 and 10 show the compared production GOR and recovery-factor curves, respectively. The formulation of the 1D foamy-oil model captures the features in the core-plug primary depletion of the foamy-oil flow in the Albania oil field. As these figures indicate, a good agreement between the experimental and simulation results is obtained for this case study as well. In the current case, the overall recovery was almost 65% of the OOIP in the core with a maximal gas saturation of 44.12% at the final 0-psi depletion condition. The recovery factor is higher than that observed in fields because of the experimental data used (Bennion et al. 2003).

Conclusions

From the experimental analysis in our first paper (Wang et al. 2008), it was shown that foamy-oil phenomena indeed exist during the development of the Orinoco-belt heavy oil in Venezuela because of the high bubblepoint pressure and solution GOR as well as the special properties of the oil. In this paper, on the basis of the pseudobubblepoint concept, a mathematical model of foamy solution-gas drive that incorporates the physics of generation and flow of gas-in-oil dispersion was obtained, and its phase behavior was systemically modeled. Through a computational code that the authors developed, this model was validated with our previous experimental results (Wang et al. 2008) and those in Bennion et al. (2003). Reasonable match results between the modeling and experimental approaches were obtained. Because the experimental results in these two earlier papers matched their corresponding field observations, the model derived in the current

TABLE 5—SUMMARY OF THE COREFLOOD EXPERIMENTAL SETUP (MAINI 1999)	
Length, cm	15.122
Area, cm^2	38.07
Temperature, K	316
Pore pressure, psi	3,300
Porosity, %	35
Permeability, md	180
Oil compressibility, psi^{-1}	5×10^{-6}
Oil density, g/cm^3	0.9785
Gas density, g/cm^3	0.9979×10^{-3}
Oil viscosity, cp	1,195
Gas viscosity, cp	0.0228

TABLE 6—EXPERIMENTAL RESULTS OF THE COREFLOOD (MASTMANN ET AL. 2001)

Cumulative Time (hour)	Pressure (psi)	ΔP (psi)	Dead-Oil Production (cm^3)	Gas Prod. (cm^3)	GOR, Incorporated (m^3/m^3)	S_g	S_o	Recovery (% OOIP)
0	3333	0.2				0	1	
17.2	3154	0.1	0.07	2.6	31.94	0	1	0.075
29.8	3023	0.5	0.05	1.8	30.96	0	1	0.128
51.1	2801	0.4	0.1	3.8	32.68	0	1	0.235
62.7	2680	0.5	0.28	9.29	33.17	0	1	0.535
79.2	2508	1.6	2.65	63.9	24.11	0.006	0.994	1.179
89.5	2401	0.3	1.27	45.15	35.55	0.022	0.978	2.676
123.2	2050	1.8	3	78.26	26.09	0.038	0.962	4.389
135.4	1923	2.3	1.27	45.15	35.55	0.042	0.958	4.731
154.2	1728	2.3	0.7	47.73	68.18	0.049	0.951	5.481
173.1	1522	1.35	0.35	30.53	87.23	0.054	0.946	6.236
196.8	1284	2.31	1.2	34.4	28.67	0.065	0.935	7.140
262.1	604	11.21	18.75	643.28	34.31	0.267	0.733	27.212
286.1	355	15	11.6	1109.4	95.63	0.311	0.689	31.601
312.2	81	22.6	5.2	838.5	161.25	0.366	0.634	37.167

paper was, in turn, validated from field data. The modeling and simulation studies performed will help the design of development and production projects for heavy-oil reservoirs.

Nomenclature

B_{fo} = formation volume factor of foamy oil
B_g = formation volume factor of gas
k = permeability
k_{rfo} = foamy-oil relative permeability
k_{rg} = gas relative permeability
m_1 = viscosity multiplier
m_2 = viscosity multiplier
p = pressure
p_b = bubblepoint pressure
p_{cgfo} = capillary pressure between foamy oil and gas phase
p_g = gas-phase pressure
p_{pb} = pseudobubblepoint pressure
p_{ref} = reference pressure
q = well rate
q_{fo} = foamy-oil-flow rate
q_g = gas-flow rate
R_{bs} = solution GOR at bubblepoint pressure
R_s = solution GOR
R_{sfo} = foamy-oil solution GOR
R_{so} = GOR
S_{fo}^{dg} = saturation of the dispersed gas
S_{fo} = foamy-oil saturation
S_g = gas saturation
T = temperature
u_{fo} = foamy-oil velocity
u_g = free-gas velocity
V_{dg} = volume of dispersed gas
V_{do} = volume of dead oil
V_{doS} = volume of dead oil at standard condition
V_g = volume of free gas
V_{gS} = volume of free gas at standard condition
V_{sg} = volume of solution gas
V_{sgS} = volume of solution gas at standard condition
α_g = entrained-gas fraction
β = volume fraction of gas entrained in the foamy-oil phase
Δz = thickness
γ_{fos} = specific gravity of stock-tank foamy oil
γ_{gs} = specific gravity of gas at stock-tank conditions
μ_{fo} = foamy-oil viscosity
μ_g = gas viscosity
μ_o = conventional oil viscosity
ϕ = porosity
ϕ_g = ratio of volume of gas flashed to the total solution volume
$\wp$ = magnitude of gravitational acceleration
ρ_{fo}^{dg} = mass density of dispersed gas

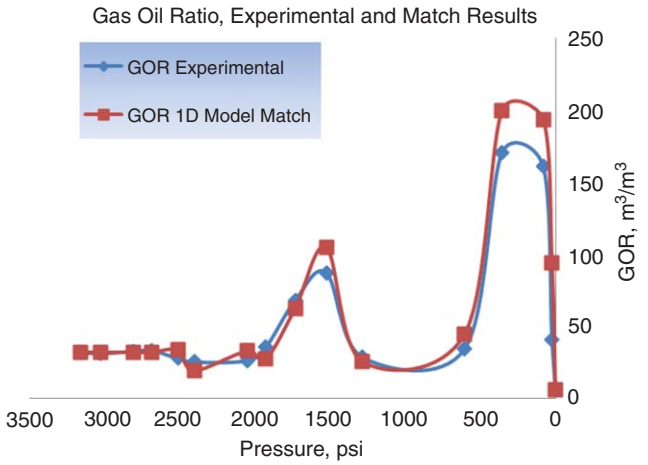

Fig. 9—Production GOR, experimental vs. simulation results.

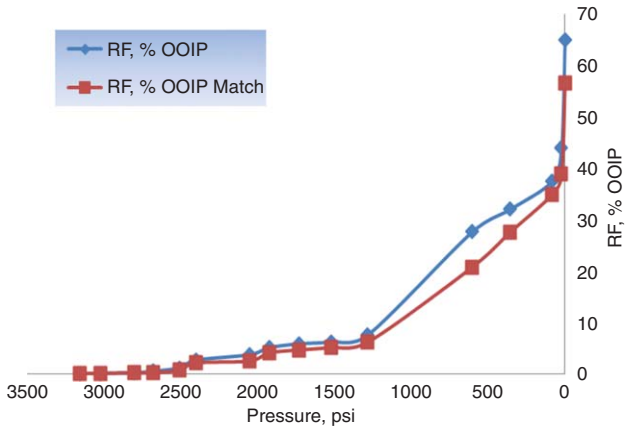

Fig. 10—Recovery in percentage of OOIP, experimental vs. simulation results.

ρ_{fo}^{do} = mass density of dead oil
ρ_{fo} = foamy-oil density
ρ_g = free-gas density
ρ_{fo}^{sg} = mass density of solution gas

Subscripts/Superscripts

dg = dispersed gas
do = dead oil
fo = foamy oil
s = standard condition
x,y,z = coordinates

References

Baibakov, N.K. and Garushev, A.R. 1989. *Thermal Methods of Petroleum Production, Developments in Petroleum Science 25*, translated by W.J. Cieslewicz, Amsterdam: Elsevier Science, 6–21.

Bennion, D.B., Mastmann, M., and Moustakis, M.L. 2003. A Case Study of Foamy Oil Recovery in the Patos-Marinza Reservoir, Driza Sand, Albania. *J Can Pet Technol* **42** (3): 21–28. PETSOC-03-03-01. http://dx.doi.org/10.2118/03-03-01 .

Chen, Z. 2006. Heavy Oils, Part I and Part II. *SIAM News*, April and May Issues.

Chen, Z., Huan, G., and Ma, Y. 2006. Computational Methods for Multiphase Flows in Porous Media. In the *Computational Science and Engineering Series*, Vol. **2**, Philadelphia, Pennsylvania: SIAM.

Claridge, E.L. and Prats, M. 1995. A Proposed Model and Mechanism for Anomalous Foamy Heavy Oil Behavior. *Proc.*, International Heavy Oil Symposium, Calgary, Alberta, Canada, 19–21 June, 9–20. SPE-29243-MS. http://dx.doi.org/10.2118/29243-MS.

Conaway, C. 1999. *The Petroleum Industry: A Nontechnical Guide*, Tulsa, Oklahoma: Pennwell Publishing Co.

Curtis, C., Kopper, R., Decoster, E. et al. 2002. Heavy Oil Reservoirs. *Oilfield Rev.* **14** (3): 30–51.

Joseph, D.D., Kamp, A.M., and Bai, R. 2002. Modeling Foamy Oil Flow in Porous Media. *International J. Multiphase Flow* **28:** 1659–1686.

Kraus, W.P., McCaffrey, W.J., and Byod, G.W. 1993. Pseudo-Bubble Point Model for Foamy Oils. Presented at the 44th Annual Technical Conference Petroleum Society of CIM, Calgary, Alberta, Canada, 9–12 May. CIM-93-45.

Kumar, R. and Mahadevan, J. 2008. Well-Performance Relationships in Heavy Foamy Oil Reservoirs. Presented at the 2008 SPE International Thermal Operations and Heavy Oil Symposium, Calgary, Alberta, Canada, 20–23 October. SPE-117447-MS. http://dx.doi.org/10.2118/117447-MS.

Lebel, J.P. 1994. Performance Implications of Various Reservoir Access Geometries. Presented at the 11th Annual Heavy Oil and Oil Sands Technical Symposium, 2 March.

Loughhead, D.J. and Saltuklaroglu, M. 1992. Lloydminster Heavy Oil Production: Why So Unusual? Presented at the 9th Annual Heavy Oil and Oil Sand Symposium, Calgary, Alberta, Canada, 11 March.

Maini, B.B. 1996. Foamy Oil Flow in Heavy Oil Production. *J Can Pet Technol* **35** (6): 21–24. SPE-96-06-01-PA. http://dx.doi.org/10.2118/96-06-01-PA.

Maini, B.B. 1999. Foamy Oil Flow in Primary Production of Heavy Oil Under Solution Gas Drive. Presented at the 1999 SPE Annual Technical Conference and Exhibition, Houston, Texas, 3–6 October. SPE-56541-MS. http://dx.doi.org/10.2118/56541-MS.

Mastmann, M., Moustakis, M., and Bennion, D.B. 2001. Predicting Foamy Oil Recovery. Presented at the SPE Western Regional Meeting, Bakersfield, California, 26–30 March. SPE-68860-MS. http://dx.doi.org/10.2118/68860-MS.

Nehring, R., Hess, R., and Kamionski, M. 1983. *The Heavy Oil Resources of the United States*, R-2946-DOE, February.

Sarma, H. and Maini, B.B. 1992. Role of Solution Gas in Primary Production of Heavy Oils. Presented at the Second Latin American Petroleum Engineering Conference, Caracas, Venezuela, 8–11 March. SPE-23631-MS. http://dx.doi.org/10.2118/23631-MS.

Sheng, J.J., Hayes, R.E., Maini, B.B. et al. 1999a. Modeling Foamy Oil Flow in Porous Media. *Transport in Porous Media* **35** (2): 227–258. http://dx.doi.org/10.1023/A:1006523526802.

Sheng, J.J., Maini, B.B., Hayes, R.R. et al. 1999b. Critical Review of Foamy Oil Flow. *Transport in Porous Media* **35** (2): 157–187. http://dx.doi.org/10.1023/A:1006575510872.

Smith, G.E. 1988. Fluid Flow and Sand Production in Heavy Oil Reservoirs Under Solution Gas Drive. *SPE Prod Eng* **3** (2): 169–180. SPE-15094-PA. http://dx.doi.org/10.2118/15094-PA.

Standing, M.B. 1981. *Volume and Phase Behaviour of Oil Field Hydrocarbon Systems*, ninth edition, Dallas, Texas: Society of Petroleum Engineers.

Tang, G.Q., Sahni, A., Gadelle, F. et al. 2006. Heavy-Oil Solution Gas Drive in Consolidated and Unconsolidated Rock. *SPE J.* **11** (2): 259–268. SPE-87226-PA. http://dx.doi.org/10.2118/87226-PA.

Tissot, B.P. and Welte, D.H. 1978. *Petroleum Formation and Occurrence*, Berlin: Springer-Verlag.

Treinen, R.J., Ring, W.W., Spence, A.P. et al. 1997. Hamaca: Solution Gas Drive Recovery in a Heavy Oil Reservoir, Experimental Results. Presented at the 5th Latin American and Caribbean Petroleum Engineering Conference and Exhibition, Rio de Janeiro, Brazil, 30 August–3 September. SPE-39031-MS. http://dx.doi.org/10.2118/39031-MS.

Tremblay, B. 2005. Modeling of Sand Transport Through Wormholes. *J Can Pet Technol* **44** (4): 51–55. PETSOC-05-04-06-PA. http://dx.doi.org/10.2118/05-04-06-PA.

Wang, R., Qin, J., Chen, Z. et al. 2008. Performance of Drainage Experiments With Orinoco Belt Heavy Oil in a Long Laboratory Core in Imitated Reservoir Conditions. *SPE J.* **13** (4): 474–479. SPE-104377-PA. http://dx.doi.org/10.2118/104377-PA.

Zhangxin Chen is a professor in the Department of Chemical and Petroleum Engineering and the Director of the Foundation CMG/Frank-Sarah Meyer Collaboration Centre, the University of Calgary. He has the distinction of holding two Chair awards: the NSERC/AIEE (AERI)/Foundation CMG Senior Research Chair in Reservoir Simulation and the Alberta Innovates: Technology Futures (AITF, formerly iCORE) Industrial Chair in Reservoir Modeling. Chen earned a PhD degree from Purdue University, and his research specialty is in reservoir modeling and simulation and scientific computing.

Jian Sun holds an MSc degree from the University of Calgary.

Ruihe Wang is a Foundation CMG Chair at China University of Petroleum, Beijing, and the deputy chief engineer in China National Oil and Gas Exploration and Development Corporation, a branch of China National Petroleum Corporation, in charge of overseas oil-development business. He earned a PhD degree in reservoir engineering from Southwest Petroleum University, Beijing. Wang's research interest is in integrated studies in enhanced oil recovery, oil-production technology, mechanics of multiphase flows in porous media, reservoir-simulation modeling, and simulator development.

Xiaodong Wu is a professor in the Faculty of Petroleum Engineering at the Petroleum University of China, Beijing. Wu is a specialist in artificial lift and wellbore vertical flow simulation.